Suppression of Kpnβ1 expression inhibits human breast cancer cell proliferation by abrogating nuclear transport of Her2

CHENYI SHENG[1*], JIAN QIU[2*], ZHIXIAN HE[1], HUA WANG[1], QINGQING WANG[1], ZENGYA GUO[3], LIANXIN ZHU[4] and QICHAO NI[1]

[1]Department of General Surgery, Affiliated Hospital of Nantong University; [2]Medical School of Nantong University, Nantong, Jiangsu 226001; [3]Department of General Surgery, Tongzhou People's Hospital, Nantong, Jiangsu 226300; [4]Department of Surgical Oncology, Lu'an People's Hospital Tumor Center, The Lu'an Affiliated Hospital of Anhui Medical University, Lu'an, Anhui 237000, P.R. China

Received April 6, 2017; Accepted October 23, 2017

DOI: 10.3892/or.2017.6151

Abstract. Breast cancer (BC) is one of the most fatal diseases and poses critical health problems worldwide. However, its mechanisms remain unclear. Consequently, there is an urgency to investigate the mechanisms involved in BC initiation and progression and identify novel therapeutics for its prevention and treatment. In this study, we identified karyopherin β-1 (Kpnβ1) as a possible novel therapeutic target for BC. Western blotting was used to evaluate the expression of Kpnβ1 in four pairs of tumorous and adjacent non-tumorous tissues. The results revealed that the protein level of Kpnβ1 was higher in the cancer samples compared with those in the corresponding normal samples. Immunohistochemistry was performed on 140 BC cases and indicated that Kpnβ1 was significantly associated with clinical pathological variables. Kaplan-Meier curve revealed that high expression of Kpnβ1 was related to poor BC patient prognosis. A starvation and re-feeding assay was used to imitate the cell cycle using the SKBR-3 cell line, indicating that Kpnβ1 plays a critical role in cell proliferation. The Cell Counting Kit-8 assay revealed that SKBR-3 cells treated with Kpnβ1-siRNA (siKpnβ1) grew more slowly than the control cells, while flow cytometry revealed that low-Kpnβ1 expressing SKBR-3 cells exhibited increased BC cell apoptosis. Furthermore, the interaction between Kpnβ1 and Her2 was clearly observed by immunoprecipitation, indicating that Kpnβ1-knockdown abrogated nuclear transport of Her2. In summary, our findings revealed that Kpnβ1 is involved in the progression of BC and may be a useful therapeutic target.

Correspondence to: Professor Qichao Ni, Department of General Surgery, Affiliated Hospital of Nantong University, Nantong, Jiangsu 226001, P.R. China
E-mail: nqcuser@163.com

*Contributed equally

Key words: Kpnβ1, breast cancer, proliferation, nuclear transport, Her2

Introduction

Breast cancer (BC) is the most commonly diagnosed cancer among women worldwide and a leading cause of cancer-related mortality in developed countries (1). According to recent research, BC has risen to have the second highest mortality rate among cancers (2). As a disease with a complex, multifarious genetic and biochemical background, the exact mechanisms of breast carcinogenesis remain unclear. Hence, screening for more useful prognostic and predictive markers that contribute to BC progression is urgently needed to identify more effective therapies.

Karyopherin (Kpn) proteins, all of which have an N-terminal RanGTP-binding domain, a C-terminal cargo-binding domain, and the capacity to bind components of the nuclear pore complex (NPC), are nuclear transport receptors that function in transporting cargo proteins and certain RNAs into and out of the cell nucleus via the NPC (3). Nuclear import via Kpn β-1 (Kpnβ1) can occur either by Kpnβ1 acting as an autonomous nuclear transport receptor, or through its association with an adaptor protein, such as Kpnα (also known as importin alpha), in which case the import process is known as classical nuclear import (4). Kpnβ1 is involved in importing proteins, such as receptor tyrosine kinase 2 (ErbB-2) (5), epidermal growth factor receptor (EGFR) (6), and fibroblast growth factor 1 (FGF1) (7). Furthermore, several studies have extended the role of Kpn proteins in the regulation of the cell cycle, mitosis, and replication (8). Notably, recent studies revealed that Kpn proteins also have a key role in various cancers. For example, Kpnα2 expression was found to be associated with gastric cancer (9), prostate cancer (10), epithelial ovarian carcinoma (11), BC (12), endometrial cancer (13), hepatocellular carcinoma (14) and esophageal squamous cell carcinoma (15). Furthermore, Kpn expression was found to be associated with several malignant tumors such as cervical cancer (16), malignant peripheral nerve sheath tumors (17), and head, neck and lung cancer (18). Accordingly, Kpnβ1 exhibits clear potential as an anticancer therapeutic target (19).

Although Kpn has been reported to be involved in chromosome stability in BC patients (20), there is no report demonstrating the function and mechanism of Kpn in the progression and prognosis of BC, to the best of our knowledge.

The tyrosine kinase receptor Her2 is amplified in 20-30% of human cancers and its overexpression has been associated with poor patient prognosis (21). Recently, evidence has highlighted that nuclear Her2 may play a more aggressive role during tumor progression (22). Nuclear Her2 has been determined to act as a transcription factor for genes such as cyclin D1, FGF2 and cyclooxygenase-2 (COX-2) (5). Despite recent research on the translocation of Her2 to the nucleus, the mechanism by which Her2 travels from the cell surface to the nucleus is unclear.

In this study we focused on Kpnβ1 expression in primary and BC cell lines, its association with clinicopathological features, and its prognostic value for BC patient survival. This study provided evidence for a role of Kpnβ1 in contributing to BC phenotype. Furthermore, we investigated the possible role of Kpnβ1 in the proliferation and apoptosis of BC cell lines. Based on our findings, we suggest that Kpnβ1 could be a novel therapeutic target for BC.

Materials and methods

Patients and tissue samples. BC sections were obtained from 140 patients who had undergone breast surgical resection at the Department of General Surgery of the Affiliated Hospital of Nantong University between April 2002 and May 2010. The tissues had been formalin-fixed and paraffin-embedded for pathological diagnosis and immunohistochemical study and were authenticated histologically. The TNM tumor staging and histological grade were performed according to the World Health Organization guidelines. Patient information corresponding with these tissues was subsequently obtained from return patient visits to the hospital and telephone contact. The clinical features of all the patients, including age, tumor size, histologic grade, axillary lymph node status, and histology are shown in Table I. Fresh BC and normal tissue samples were immediately frozen in liquid nitrogen after surgical resection and maintained at -80˚C. All human tissues were collected using protocols approved by the Ethics Committee of the Affiliated Cancer Hospital of Nantong University (Nantong, Jiangsu, China). The median patient age was 54 years (range, 34-88 years). The median 7-year follow-up time for the 140 patients was 30 months (range, 6-90 months). Histological grade was classified as follows: well-differentiated (grade I, n=17), moderately differentiated (grade II, n=60), and poorly differentiated (grade III, n=63). The majority of cases included infiltrating ductal carcinoma (n=109, 78%) and the remaining 22% of the cases consisted of other types. The main patient clinicopathological variables are shown in Table I. Informed consent was obtained from all patients.

Table I. Expression of Kpnβ1, Ki-67 and clinicopathological parameters in 140 breast cancer specimens.

		Kpnβ1 expression			
Parameters	Total	Low	High	P-value[a]	χ^2
Age (years)					
≤50	57	28	29	0.975	0.001
>50	83	41	42		
Grade					
I	17	11	6	0.048[a]	6.081
II	60	34	26		
III	63	24	39		
ER					
Negative	69	36	33	0.500	0.454
Positive	71	33	38		
PR					
Negative	70	34	36	0.866	0.029
Positive	70	35	35		
Her2					
Negative	68	38	30	0.129	2.203
Positive	72	31	41		
Tumor size					
≤2x2x2	77	41	26	0.007[a]	7.290
>2x2x2	63	28	45		
Axillary lymph node status					
N0	52	31	21	0.060	3.532
Nx	88	38	50		
Nerve invasion and metastasis					
Negative	85	45	40	0.282	1.157
Positive	55	24	31		
Vascular metastasis					
Negative	75	42	33	0.088	2.914
Positive	65	27	38		
Histology					
Ductal	109	59	50	0.032[a]	4.619
Others	31	10	21		
Ki-67					
Low	49	18	31	0.015[a]	5.894
High	91	38	53		

[a]Statistical analyses were performed by Pearson's χ^2 test. P<0.05 was considered as statistically significant. Kpnβ1, karyopherin β-1; ER, estrogen receptor; PR, progesterone receptor.

Antibodies. All antibodies were sourced from Santa Cruz Biotechnology (Santa Cruz, CA, USA) unless otherwise specified. Antibodies for immunohistochemistry included anti-Kpnβ1 (sc-11367, 1:200) and anti-Ki-67 (AB9260, 1:100; Millipore, Bedford, MA, USA); for western blot analysis they included anti-Kpnβ1 (1:500), anti-proliferating cell nuclear antigen (PCNA; 1:1,000), anti-β-actin antibody (1:1,000), anti-cyclin D1 antibody (1:1,000) and anti-GAPDH (sc-7196, 1:1,000); and for immunofluorescent staining they included anti-Kpnβ1 (1:500), anti-Her2 (1:400), and anti-actin monoclonal antibody (1:1,000).

Immunohistochemical staining. In brief, tissue slices were dewaxed in xylene, rehydrated in graded ethanol and endogenous peroxidase activity was blocked by steeping in 3% methanolic peroxide for 20 min. The sections were then heated to 121˚C in an autoclave for 10 min in 0.1 M citrate buffer (pH 6.0) to retrieve the antigen. After being rinsed in phosphate-buffered saline (PBS, pH 7.2) for 5 min (three times), tissue sections were incubated with the rabbit anti-human Kpnβ1 antibody (diluted 1:200) and the mouse anti-human Ki-67 antibody (diluted 1:500) for 3 h at room temperature. After being washed with PBS, the peroxidase reaction was visualized by incubating the sections with DAB [0.1% phosphate-buffered solution (PBS), 0.02% diaminobenzidine tetrahydrochloride, and 3% H_2O_2]. Finally, the sections were counterstained with hematoxylin, dehydrated through graded alcohol, and mounted under a cover slip after being rinsed in water.

Immunohistochemical evaluation. All immunostained sections were randomly evaluated by three independent observers in a blinded manner using a Leica fluorescence microscope (Leica Microsystems GmbH, Wetzlar, Germany). Five fields of view were chosen per slide and at least 500 cells were counted per view at high power. To evaluate the immunoreaction of Kpnβ1, the staining intensity was estimated in comparison to the control and scored as follows: I, the reaction was not easily perceived from the background or <5% of tumor cells were stained; II, 5-30% of tumor cells were positively stained; and III, >30% of tumor cells were positively-stained (Xue *et al*, 2013).

Western blot analysis. Before immunoblotting, tissues were immediately homogenized in lysis buffer [1% NP-40, 50 mmol/l Tris (pH 7.5), 5 mmol/l EDTA, 1% SDS, 1% sodium deoxycholate, 1% Triton X-100, 1 mmol/l PMSF, 10 mg/ml aprotinin and 1 mg/ml leupeptin] and the cells were washed three times with ice-cold PBS and resuspended in 2X lysis buffer (50 mM Tris-HCl, 120 mM NaCl, 0.5% NP-40, 100 mM NaF, 200 mM Na_3VO_4, and protease inhibitor mixture). The cells were then denatured at 100˚C for 15 min. Total protein concentration was then determined with a Bio-Rad protein assay (Bio-Rad Laboratories, Hercules, CA, USA). All protein samples were stored at -20˚C. For sodium dodecyl sulfate-polyacrylamide gel electrophoresis (SDS-PAGE), samples were denatured at 100˚C for 3 min. The proteins were then separated with SDS-PAGE and subsequently transferred to polyvinylidene difluoride filter (PVDF) membranes (Millipore). The membranes were then blocked in 5% skimmed-milk in Tris-buffered saline-Tween (TBST: 20 mM Tris, 150 mM NaCl, 0.05% Tween-20) for 2 h at room temperature, and then incubated with primary antibodies overnight at 4˚C for 6-8 h at room temperature. The membranes were then washed with TBST three times (5 min/wash) and incubated with horseradish peroxidase-linked IgG secondary antibodies for 2 h at room temperature. The protein bands were detected using the enhanced chemiluminescence (ECL) detection system (Pierce, Rockford, IL, USA) and the band intensities were assessed using ImageJ analysis software (Wayne Rasband; National Institutes of Health, Bethesda, MD, USA).

Cell culture and cell cycle analysis. Two human BC cell lines, SKBR-3 and MDA-MB-231, were obtained from the Cell Bank of the Chinese Academy of Sciences (Shanghai, China) and used in this study. The MDA-MB-231 cell line was maintained in Dulbecco's modified Eagle's medium (DMEM; Gibco-BRL, Grand Island, NY, USA) supplemented with 10% heat-inactivated fetal bovine serum (HI-FBS), 2 mM L-glutamine, and 100 U/ml penicillin-G and incubated at 37˚C and 5% CO_2. The SKBR-3 cell line was maintained in Mccoy's 5A medium (Gibco-BRL) supplemented with 10% HI-FBS, 2 mM L-glutamine, and 100 U/ml penicillin-G and incubated at 37˚C and 0% CO_2.

Starvation and re-feeding was used to imitate the cell cycle. First, DMEM or Mccoy's 5A medium without FBS was used to incubate the MDA-MB-231 or SKBR-3 cells, respectively, for 48 h to synchronize cells, and was then replaced by complete medium. Subsequently, the cells were rapidly harvested at specified time-points and fixed in 70% ethanol for at least 24 h at -20˚C, and then incubated with 1 mg/ml RNase A for 20 min at 37˚C. The cells were then stained with 0.5% Tween-20/propidium iodide (PI, 50 mg/ml) in PBS and analyzed using a Becton-Dickinson flow cytometer (BD FACScan; Becton-Dickinson, San Jose, CA, USA) and CellQuest acquisition and analysis programs.

RNA interference of Kpnβ1. Small interference RNAs (siRNA) were designed and chemically synthesized by GeneChem (Shanghai, China). The Kpnβ1-specific siRNA target sequences were as follows: Kpnβ1-siRNA#0, 5'-GAGATCGAAGACTA ACAAA-3'; Kpnβ1-siRNA#1, 5'-CAGTGTAGTTGTTCGA GAT-3'; Kpnβ1-siRNA#2, 5'-ACGAGAAGTCAAGAAC TAT-3'; and non-specific scrambled siRNA sequence, 5'-GCTGTTAGTGAGCTAAGTA-3'. Cells were transfected with 100 nmol/l of siRNA duplexes using Lipofectamine Plus reagent (Invitrogen, Carlsbad, CA, USA) according to the manufacturer's protocol.

Plate colony formation assay. SKBR-3 and MDA-MB-231 cells pretreated with Kpnβ1-siRNA and non-specific scrambled siRNA (2,000 cells/plate) were cultured in 5 ml of DMEM supplemented with 10% FBS in a 6-cm plate. After 14 days, the colonies were washed with PBS, fixed with methanol for 30 min, and stained with crystal violet for 30 min. Clearly visible colonies (>50 mm in diameter) were counted as positive for growth.

Cell proliferation assay. Cell Counting Kit-8 (CCK-8; Dojindo Laboratories, Kumamoto, Japan) was employed to assess cell proliferation. In brief, the cells were seeded into a 96-well cell culture cluster plate (Corning Incorporated, Corning, NY, USA) at a concentration of $2x10^4$ cells/well in a volume of 100 μl and grown overnight. The cells were then incubated with CCK-8 reagents for 2 h at 37˚C and the absorbance was quantified on an automated plate reader. Each condition was performed in triplicate and each experiment was repeated three times.

Flow cytometric analysis of cell apoptosis. SKBR-3 cells transfected with Kpnβ1-siRNA and control-siRNA were cultured for 48 h and harvested. Muse™ Annexin V and

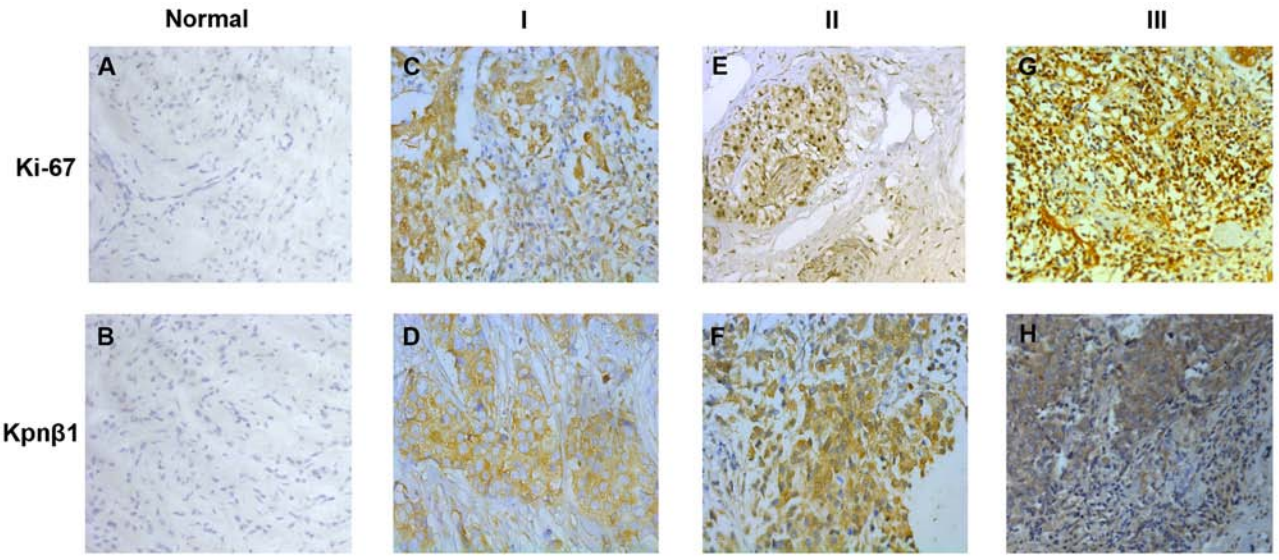

Figure 1. Immunohistochemical staining of Kpnβ1 and Ki-67 expression in paraffin-embedded BC tissues. (A and B) Kpnβ1 and Ki67 staining in BC tissues and adjacent normal tissues. Expression levels of Kpnβ1 and Ki-67 were (C and D) low (weakly positive) in grade I tissues; (E and F) moderate in grade II tissues; and (G and H) high in grade III tissues. The images in A-H were captured at x400 magnification. BC, breast cancer; Kpnβ1, karyopherin β-1.

Dead Cell reagent (60 μl, part no. 4700-1485, 100 tests/bottle) was then added to each tube with 60 μl of cell suspension. After incubation for 20 min at room temperature in the dark, the apoptosis assay was performed using the Muse™ Cell Analyzer (Millipore) according to the manufacturer's instructions.

Coimmunoprecipitation. Cellular extracts were lysed in lysis buffer (150 mM NaCl, 1 mM EDTA, 20 mM Tris (pH 7.5), 0.5% NP-40, 1 mM NaF, 1 mM MNa_3VO_4, 1 mM PMSF, and 2 g/ml aprotinin) and incubated with primary antibodies at 4˚C followed by incubation with protein G-sepharose. The immunocomplexes were washed three times with lysis buffer. For single immunoprecipitation, the bound proteins were eluted by boiling the samples in SDS sample buffer containing 2-mercaptoethanol. For sequential double immunoprecipitation, the bound proteins were eluted from the sepharose beads by boiling for 3 min in 25 l of SDS lysis buffer (20 mM Tris (pH 7.5), 50 mM NaCl, 1% SDS, and 1 mM dithiothreitol). Samples were cooled and the supernatants were diluted with 225 l of lysis buffer containing the appropriate antibodies and incubated overnight at 4˚C. The immunocomplexes were then precipitated with protein A-Sepharose beads, washed with lysis buffer, and resuspended in SDS sample buffer. The eluted proteins were then boiled for 5 min and subjected to SDS-PAGE.

Immunofluorescent staining assay. Following prior treatment, the cells were fixed with paraformaldehyde for 40 min at room temperature, permeabilized for 15 min with 1% Triton-X, blocked for 2 h with 1% BSA in PBS at 4˚C, and incubated overnight at 4˚C with anti-Kpnβ1 monoclonal and anti-Her2 antibodies. The cells were then washed three times with PBS followed by incubation for 2 h with anti-rabbit IgG secondary antibody, anti-mouse IgG secondary antibody, or anti-actin monoclonal antibody. Nuclear staining was achieved with DAPI (4,6-diamidino-2-phenylindole; fluorescence) before mounting. After being washed with PBS, the slides were air-dried, mounted with anti-fading mounting reagent, and examined under a fluorescent microscope.

Statistical analysis. Data were analyzed by SPSS 17.0 software (SPSS, Inc., Chicago, IL, USA). Statistical significance of the correlations between Kpnβ1 and Ki-67 expression and the clinicopathological features were analyzed using the Chi-squared test. The Kaplan-Meier method was used to analyze survival curves and the log-rank test. Multivariate analysis was performed using Cox's proportional hazards model. The results are expressed as means ± standard deviation (SD). $P<0.05$ was considered to indicate a statistically significant result.

Results

The expression of Kpnβ1 and Ki-67 in human malignant breast tissues and cell lines. To identify whether Kpnβ1 was associated with BC, immunohistochemistry was applied to detect the expression and distribution of Kpnβ1 and Ki-67 in paraffin-embedded mammary tissue sections screened from 140 patients. For statistical analysis of Kpnβ1 and Ki-67 expression levels, we defined Kpnβ1 antibody specificity and scored Kpnβ1 staining as weakly positive (I), moderately positive (II), and strongly positive (III) based on the percentage of positively stained cells and staining intensity. When considering the characteristics of the data, we then classified group I as low expression and groups II and III as high expression. The results of these experiments revealed that Kpnβ1 was mainly located in the cytoplasm with high expression of Kpnβ1 significantly consistent with high expression of nuclear Ki-67 (Fig. 1).

To verify whether Kpnβ1 is highly expressed in human BC, we further detected the expression of Kpnβ1 by western blot analysis in four pairs of fresh samples. As shown in Fig. 2A and B, the expression of Kpnβ1 was much higher in

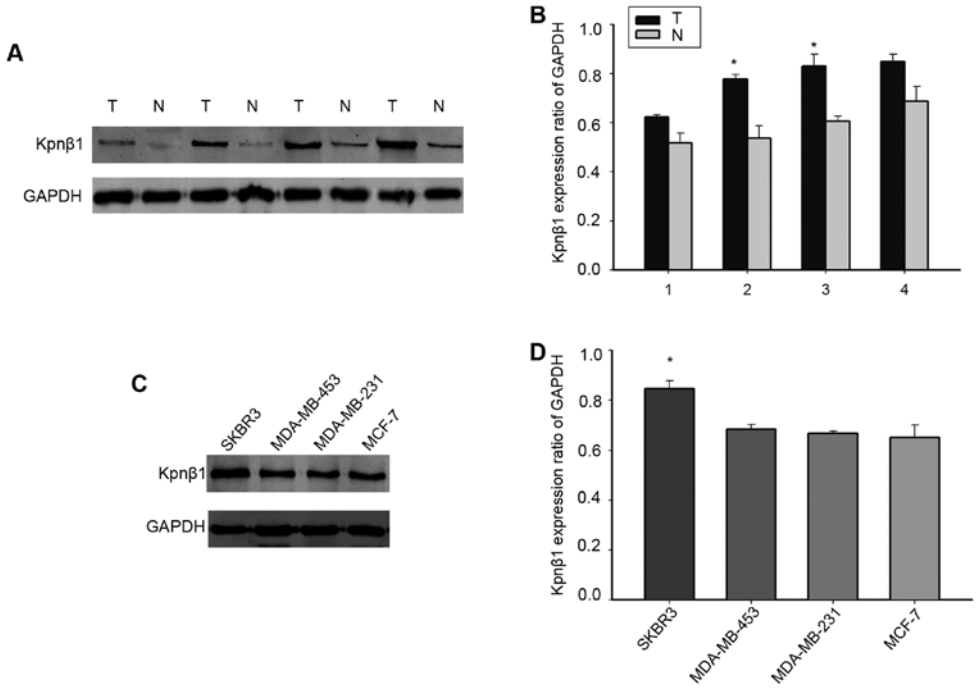

Figure 2. Kpnβ1 expression in BC tissues. Kpnβ1 expression levels in four paired adjacent normal and breast carcinoma tissues assessed by (A) western blotting and (B) density photometry. Expression of Kpnβ1 in four BC cell lines analyzed by (C) western blotting and (D) density photometry. The data from each time point were derived from three independent experiments. *P<0.05. T, tumor; N, adjacent normal tissues; BC, breast cancer; Kpnβ1, karyopherin β-1.

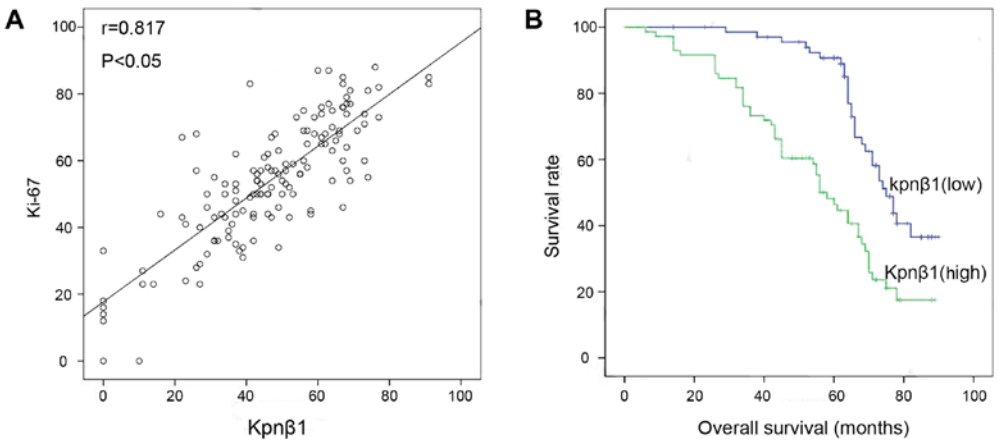

Figure 3. (A) The relationship between the Ki-67 proliferation index and Kpnβ1 expression in breast carcinoma tissues. Scatter plot of Ki-67 vs/ Kpnβ1 expression, with a regression line showing a significant correlation according to Spearman's correlation coefficient. (B) Association of Kpnβ1 with patient prognosis in BC. Kaplan-Meier survival curves revealed that low expression of Kpnβ1 is correlated with long-term survival. BC, breast cancer; Kpnβ1, karyopherin β-1.

malignant tumors when compared with that noted in the adjacent normal tissues, consistent with our previous observation. To further detect the expression of Kpnβ1 in BC cell lines, we selected SKBR-3, MDA-MB-453, MCF-7, and MDA-MB-231 cells. Kpnβ1 was expressed to a greater extent in SBKR-3 cells compared with the other cell lines (Fig. 2C and D). SKBR-3 cells were therefore used for subsequent experimentation. We supposed that the expression of Kpnβ1 may be related to the proliferation of BC based on these results.

The relevance of Kpnβ1 expression with clinicopathological variables and BC patient survival. To further examine the pathophysiological significance of Kpnβ1 with respect to tumor characteristics and behavior, the clinicopathological data were summarized and are shown in Table I. We found that Kpnβ1 expression was markedly correlated with grade (P=0.048), tumor size (P=0.007), histology (P=0.032), and Ki-67 expression (P=0.015). Whereas there was no association between Kpnβ1 and age (P=0.975), estrogen receptor (ER) (P=0.500), progesterone receptor (PR) (P=0.866), Her2 expression (P=0.129), axillary lymph node status (P=0.060), nerve invasion and metastasis (P=0.282) and vascular metastasis (P=0.088). Furthermore, the relationship between the Ki-67 proliferation index and Kpnβ1 expression in breast carcinoma tissues revealed a significant correlation according to Spearman's correlation coefficient (Fig. 3A). We next sought to understand the correlation between Kpnβ1 expression level and patient survival using Kaplan-Meier analysis. At the end

Table II. Survival status and clinicopathological parameters of the 140 breast carcinomas specimens.

Parameters	Total	Survival status		P-value[a]	χ^2
		Alive	Dead		
Age (years)					
≤50	57	22	35	0.325	0.968
>50	83	39	44		
Grade					
I	17	13	4	0.004[a]	11.310
II	60	28	32		
III	63	20	43		
ER					
Negative	69	35	34	0.092	2.832
Positive	71	26	45		
PR					
Negative	70	30	40	0.865	0.029
Positive	70	31	39		
Her2					
Negative	68	28	40	0.579	0.308
Positive	72	33	39		
Tumor size					
≤2x2x2	77	33	34	0.194	1.687
>2x2x2	63	28	45		
Axillary lymph node status					
N0	52	34	18	0.000[a]	16.010
Nx	88	27	61		
Nerve invasion and metastasis					
Negative	85	46	39	0.002[a]	9.788
Positive	55	15	40		
Vascular metastasis					
Negative	75	48	27	0.000[a]	27.419
Positive	65	13	52		
Histology					
Ductal	109	50	59	0.303	1.059
Others	31	11	20		
Ki-67					
Low	49	28	21	0.017[a]	5.647
High	91	33	58		
Kpnβ1					
Low	69	39	30	0.002[a]	9.281
High	71	22	49		

[a]Statistical analyses were performed by Pearson's χ^2 test. P<0.05 was considered as statistically significant. Kpnβ1, karyopherin β-1; ER, estrogen receptor; PR, progesterone receptor.

of the clinical follow-up, survival analysis was restricted to 140 patients with complete follow-up data and results for

Table III. Contribution of various potential prognostic factors to survival by Cox regression analysis in 140 breast carcinoma specimens.

Parameters	Hazard radio	95.0% CI	P-value
Kpnβ1	2.925	1.716-4.984	0.001[a]
Ki-67	0.861	0.496-1.495	0.596
Age (years)	0.919	0.569-1.483	0.729
Histology	0.698	0.402-1.210	0.200
Grade	2.121	1.384-3.251	0.001[a]
ER	0.992	0.541-1.821	0.980
PR	1.207	0.653-2.230	0.548
Her2	0.554	0.320-0.959	0.035[a]
Tumor size	0.792	0.487-1.288	0.348
Axillary lymph node status	4.065	2.212-7.469	0.001[a]
Nerve invasion and metastasis	1.078	0.635-1.829	0.780
Vascular metastasis	1.830	1.064-3.147	0.029[a]

Statistical analyses were performed by the log-rank test. [a]P<0.05 was considered as statistically significant. CI, confidence interval; Kpnβ1, karyopherin β-1; ER, estrogen receptor; PR, progesterone receptor.

Kpnβ1 expression by immunohistochemistry. Kaplan-Meier survival curves revealed that high expression of Kpnβ1 was significantly associated with poor overall survival (Fig. 3B). In addition, in the univariate analysis, when all variables were compared separately to survival status, tumor grade (P=0.004), axillary lymph node status (P=0.000), nerve invasion and metastasis (P=0.002), vascular metastasis (P=0.000), Ki-67 expression (P=0.017), and Kpnβ1 expression (P=0.002) were prognostic factors for overall survival (Table II). Multivariate analysis using the Cox's proportional hazards model indicated that Kpnβ1 expression (P=0.001), grade (P=0.001), Her2 expression (P=0.035), axillary lymph node status (P=0.001), and vascular metastasis (P=0.029) were independent prognostic indicators of overall survival (Table III).

Kpnβ1 expression is positively correlated with cell proliferation and its expression is cell-cycle dependent. Since the expression of Kpnβ1 was significantly correlated with Ki-67 expression, a cellular marker for proliferation in BC specimens, we hypothesized that Kpnβ1 may play a role in the cell cycle progression of BC cells. We demonstrated that the expression of Kpnβ1 was high in BC cells, especially in SKBR-3 cells (Fig. 2C and D). To ascertain that Kpnβ1 was invovled in the cell cycle, SKBR-3 cells were subjected to serum starvation and re-feeding. Flow cytometric analysis revealed that after 48 h serum deprivation, SKBR-3 cells were arrested in the G1 phase (86.56%). Upon re-feeding, the cells excited at the G1 phase and gradually entered S phase over time (Fig. 4A and B). We then employed western blotting to examine whether the expression of Kpnβ1 was cell-cycle dependent. Kpnβ1 expression was found to increase gradually after serum stimulation with increased time, consistent with the expression of the proliferation marker PCNA (Fig. 4C and D).

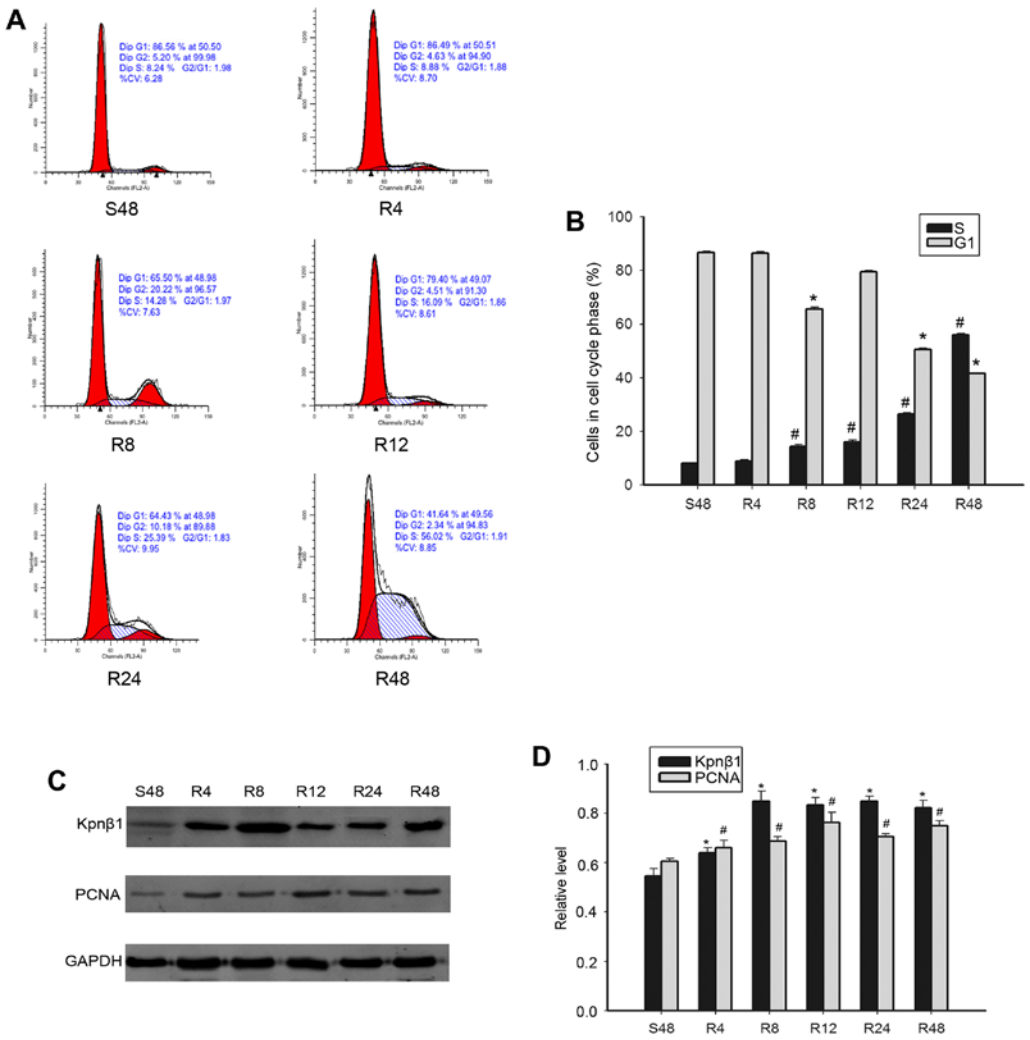

Figure 4. Expression of Kpnβ1 and cell cycle-related molecules detected in proliferating MDA-MB-231 cells by flow cytometry. (A and B) Cells synchronized at the phase G1 progressed into the cell cycle when serum was added for S48h, R4h, R8h, R12h, R24h, and R48h. (C and D) S48h MDA-MB-231 cells were released by re-feeding with serum and cell lysates were prepared and analyzed by western blotting using antibodies against Kpnβ1, PCNA, and GAPDH (loading control). Bar charts revealing the ratio of Kpnβ1, PCNA, and GAPDH by densitometry. Data are expressed or presented as the means ± SEM. $^{*,\#}$P<0.05, compared with the control cells that were serum starved for 48 h (S48h). SEM denotes the standard error of the mean. S denotes serum starvation. R denotes serum release. Kpnβ1, karyopherin β-1; PCNA, proliferating cell nuclear antigen.

These findings indicated that Kpnβ1 may play an important role in cell proliferation of SKBR-3 cells via involvement in the cell cycle.

Kpnβ1 knockdown inhibits cellular proliferation and promotes cell cycle arrest. To further verify the effect of Kpnβ1 on BC cell proliferation, chemically synthesized siRNA was employed to knock down endogenous Kpnβ1 in SKBR-3 cells. SKBR-3 cells were transfected with Kpnβ1-siRNA (siRNA-0, siRNA-1, siRNA-2) and negative control siRNA, and then the expression of Kpnβ1 was assessed by western blotting 48 h post-transfection (Fig. 5A). The results revealed that Kpnβ1 expression levels were decreased in the SKBR-3 cells transfected with Kpnβ1-siRNA compared with cells transfected with the negative control siRNA, with siRNA-2 achieving the most marked knockdown efficiency (Fig. 5A and B).

In the colony formation assay, we observed that SKBR-3 and MDA-MB-231 cell proliferation was significantly inhibited in the cells treated with siRNA-2, and was more significant in the SKBR-3 cells (Fig. 5C). This indicated that in SKBR-3 cells, the effect of Kpnβ1 on cell proliferation was more significant. Furthermore, the CCK-8 assay found that the rate of SKBR-3 cell proliferation after treatment with siRNA-2 exhibited a significant decline compared with the negative control siRNA (Fig. 5D). Additionally, flow cytometric analyses of the cell cycle in SKBR-3 cells transfected with different treatments revealed a significant increase in the G1 phase and a marked decrease in the S phase, suggesting that downregulation of Kpnβ1 arrested the cell cycle (Fig. 5E). Based on these findings, Kpnβ1-knockdown exhibited a specific inhibitory effect on cell proliferation associated with cell cycle arrest in the SKBR-3 cells.

Kpnβ1 interacts with Her2 and suppression of Kpnβ1 expression abrogates Her2 nuclear transport. Despite a lack of statistical correlation between the expression of Kpnβ1 and Her2 detected in our 140 BC tissues (P=0.129), we investigated the association between Kpnβ1 and Her2. We hypothesized that Kpnβ1-knockdown may suppress BC cell proliferation by blocking Her2 nuclear entry, and we assessed

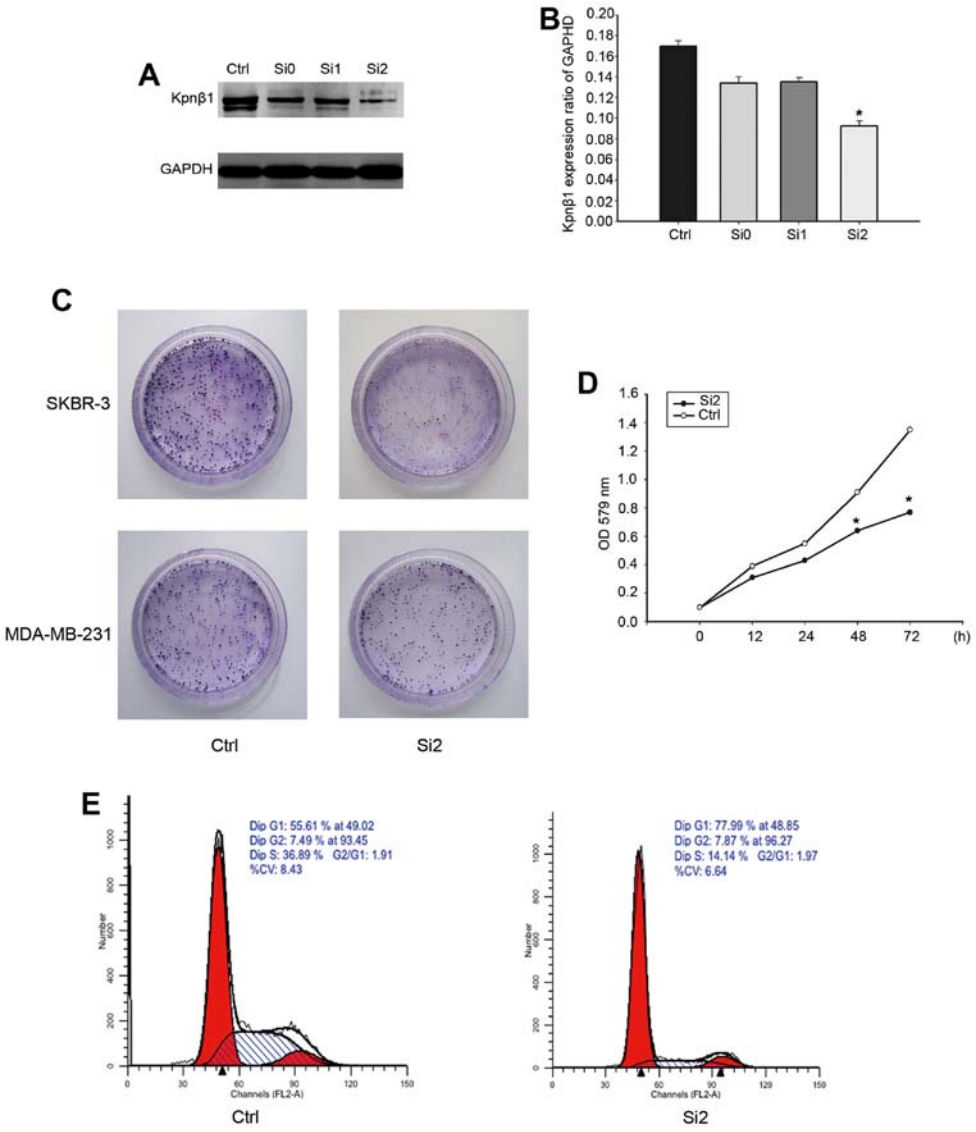

Figure 5. Kpnβ1 knockdown inhibits SKBR-3 cell proliferation *in vitro*. (A) Expression of the Kpnβ1 protein in SKBR-3 cells detected by western blotting 48 h after transfection. Transfected cells were subjected to western blot analysis with antibodies against Kpnβ1 and GAPDH (loading control). (B) Bar chart revealing the ratio of Kpnβ1 to GAPDH assessed by densitometry. Data are presented as the means ± SD, *P<0.05 compared with the control. (C) The selected and stably-transfected cells were cultivated into 6-cm culture plates and incubated for 12 days at 37˚C with 5% CO_2. Giemsa solution was used to observe diversity in the Kpnβ1-depleted cells. (D) Cell proliferation determined by the CCK-8 assay revealed that Kpnβ1-knockdown inhibited cell proliferation. CCK-8 reagents were added to the medium and incubated for an additional 2 h and the absorbance was assessed at each of the indicated time-points (0, 12, 24, 48 and 72 h). Data from each time-point were derived from three independent experiments. The data are presented as the means ± SD, *P<0.05. (E) Kpnβ1 expression was knocked down in MDA-MB-231 cells transfected with Kpnβ1-siRNA#2. The adherent cells were collected and examined by flow cytometry, which revealed a delay in G1-S transition and significant arrest at the G1 phase. Data are presented as the means ± SD. The results are a combination of the data from three independent experiments. Kpnβ1, karyopherin β-1; CCK-8, Cell Counting Kit-8.

this using the SKBR-3 cell line (Her2-overexpressing cells) The results confirmed the effect of Kpnβ1 on Her2 in SKBR-3 cells (Fig. 6A). Furthermore, immmunofluorescence detected co-localization of Kpnβ1 and Her2 in the SKBR-3 cell cytoplasm (Fig. 6B).

We next found that the localization of Her2 was affected by Kpnβ1-knockdown. When SKBR-3 cells were transfected with Kpnβ1-siRNA2, confocal microscopy demonstrated the distinct localization of Her2 in the cytoplasm and at the cell surface, but not in the nucleus as observed in the control siRNA-treated cells (Fig. 6C and D). These results indicated that Kpnβ1-knockdown abrogated nuclear transport of Her2. From the above mentioned results, we speculated that Kpnβ1 stimulated cell proliferation by promoting the nuclear translocation of Her2. However, it was not determined whether cell proliferation depended on Her2 status. Thus, we used trastuzumab to inhibit the activity of the cell membrane surface Her2. The results revealed the Her2 activities of different cases. Kpnβ1 knockdown also inhibited cellular proliferation (Fig. 6E). Therefore, Kpnβ1 interacted with Her2, then promoted nuclear transport of Her2, which was not dependent on the state of Her2.

Discussion

BC is the leading form of cancer in women, and although substantial progress has been made in its screening and management, globally it has the highest mortality rate (23).

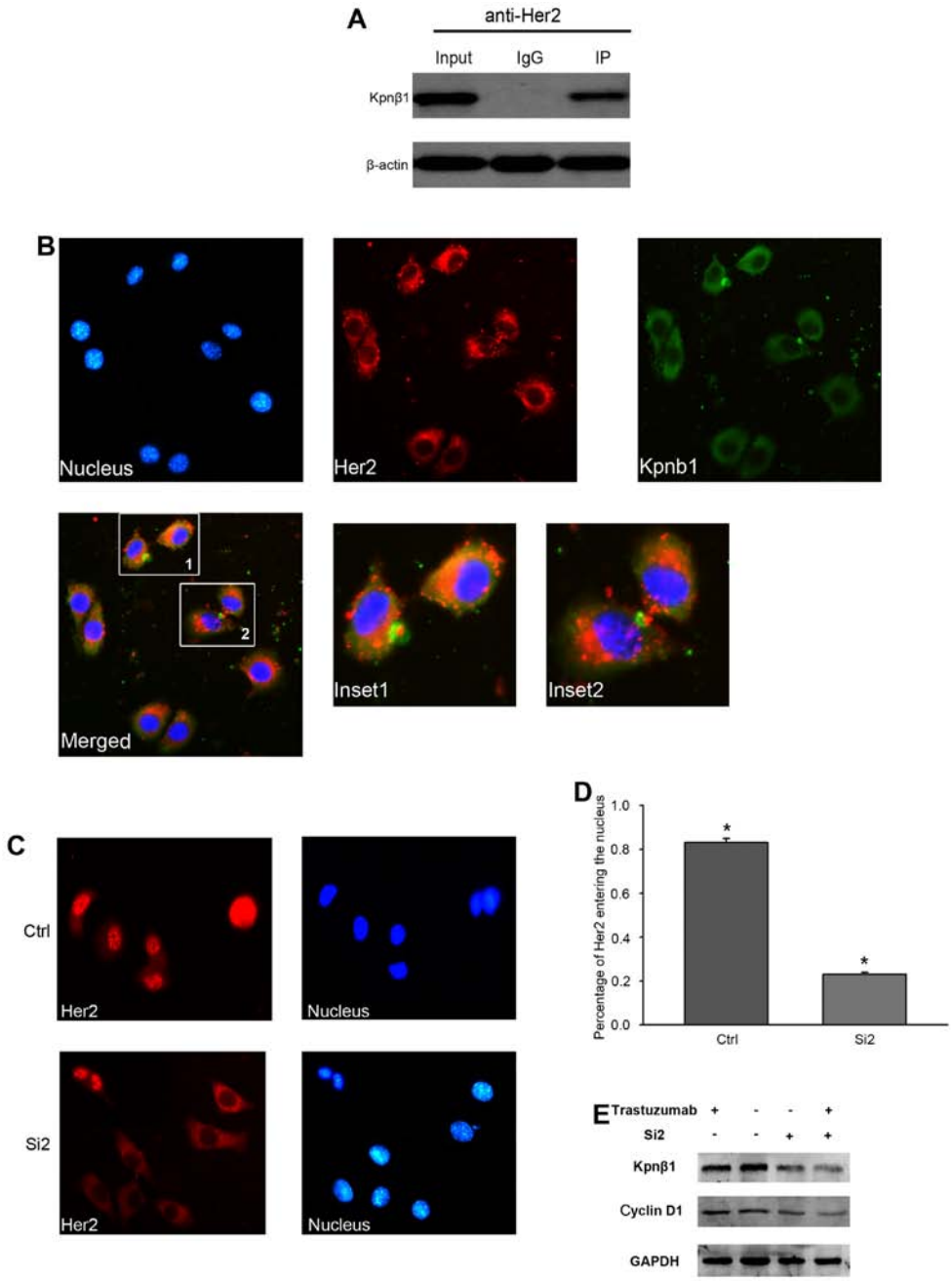

Figure 6. Kpnβ1 interacts with Her2 and suppression of Kpnβ1 expression abrogates nuclear transport of Her2. (A) SKBR-3 cells were immunoprecipitated (IP) with antibodies against Her2 or control IgG (IgG). The presence of Kpnβ1 in the immunocomplexes was examined by immunoblotting analysis. Input was used as the positive control. (B) Kpnβ1 and Her2 colocalized in the cytoplasm and the nucleus of SKBR-3 cells as shown by immunofluorescence staining (insets 1 and 2, respectively). Images were then analyzed by confocal microscopy. Boxed areas are shown in detail in insets 1 and 2. (C) Immunofluorescence staining using anti-Her2 antibody in SKBR3 cells revealed that Her2 localization changed after knockdown of Kpnβ1 expression (Si2). (D) Bar chart showing the percentage of Her2 entering the nucleus. Data are presented as the means ± SD, $^{*}P<0.05$ compared with the control. (E) Western blotting analyzed the expression of cyclin D1 to confirm whether knockdown of Kpnβ1 or trastuzumab treatment affected the proliferation of the SKBR-3 cells. Kpnβ1, karyopherin β-1.

Although BC is presently incurable, it has the potential to become curable, or at least have improved prognostics when detected at an early stage. Thus a deeper understanding of the molecular events associated with BC is essential to develop novel treatments. In this study, we identified and characterized Kpnβ1 as an important player in BC progression. Kpnβ1 appears to be involved in the process of BC cell proliferation, partially by participating in the nuclear transport of Her2.

Kpnβ1 functions as a transportation cargo protein into and out of the cell nucleus during a selective, multistep process (24). Kpnβ1-mediated nuclear transportation is involved in multiple biological processes such as insulin resistance, circadian rhythm and viral infections. Kpnβ1 was found to promote palmitate-induced insulin resistance via NF-κB signaling in hepatocytes (25), and mediate PER/CRY nuclear translocation and therefore circadian clock function (26). Upregulation of Kpnβ1 was effective in nuclear localization signaling for the minor capsid proteins, VP2 and VP3, during BKPyV nuclear entry (27). Moreover, Kpnβ1 likely plays a key role in the inflammation process (28).

Studies on the effect of Kpnβ1 expression on tumors have been recently reported. There is a consensus that increased expression of certain Kpnβ proteins in cancer cells results in increased nuclear transport efficiency, thus facilitating increased oncogenic signaling and promoting the cancer phenotype (19). Increased expression of Kpnβ1 was recognized in malignant BC cells and Kpnβ1 knockdown has been shown to decrease nuclear import efficiency in malignant but not in non-transformed cells (29). Furthermore, previous studies have revealed that Kpnβ1 is overexpressed in colon, breast, lung, ovarian, and cervical cancer specimens when compared with normal tissues (17).

Many articles exist on the close relationship between Kpnβ1 expression and tumor proliferation, and Kpnβ1 inhibition has been shown to prolong mitotic arrest and apoptosis in cervical cancer cells (30). Furthermore, Kpnβ1 knockdown abrogated nuclear transport of DR5 and increased its cell surface expression. Kpnβ1-mediated nuclear localization of DR5 limited DR5/TRAIL-induced cell death of human tumor cells (31), suggesting that the molecular mechanism of Kpnβ1 and tumor proliferation was related to its mediated nuclear entry efficiency. Therefore, inhibition of Kpnβ1 represents a novel therapeutic approach for the treatment of cancer (32).

A previous study reported that the regulation of Kpnβ1 expression in cancer cells was related to the level of EZH2/miR-30a. Inhibition of E2F in cancer cells caused increased activation of Kpnβ1 promoters, leading to elevated levels of Kpnβ1 proteins, and ultimately impacting the phenotype in cervical carcinoma (33). In malignant peripheral nerve sheath tumor (MPNST) cells, EZH2 expression was significantly upregulated and the miR-30a level was significantly increased in EZH2-knockdown cells, which may inhibit the expression of Kpnβ1. Based on this, EZH2 regulated miR-30a targeted Kpnβ1 in MPNST cells (34). However, limited studies exist describing the overexpression of Kpnβ1 in BC. Consequently the molecular mechanism of Kpnβ1 remains unclear.

In our study, the expression of Kpnβ1 in SKBR-3 cells was higher than that in MDA-MB-231 cells (Fig. 2C). Although siRNA induced inhibition of Kpnβ1 in both cell lines, the effect on SKBR-3 cell proliferation was greater than that in MDA-MB-231 cells (Fig. 5C). Considering SKBR-3 cells are Her2-overexpressing BC cells and MDA-MB-231 cells are triple-negative BC cells, we hypothesized that Kpnβ1 is closely related to Her2. Previous studies have highlighted Kpnβ1-mediated Her2 nuclear entry in MCF-7/HER18 BC cells (5).

A study on the association between tumors and Her2 nuclear entry have recently increased. After Her2 nuclear entry, the transcription and expression of the ribosomal RNA (rRNA) transcription factor is accelerated, thus fostering BC protein translation and stimulating tumor proliferation and development (22). In another study, inhibition of Her2 nuclear entry reduced the expression of cyclin D1, thus decreasing the growth of BC cells (35). Therefore, we hypothesized that Kpnβ1 overexpression could increase Her2 nuclear entry, thus promoting BC proliferation, while Kpnβ1-knockdown could decrease this proliferation by blocking Her2 nuclear entry.

In this study, we identified that high expression of Kpnβ1 in BC often leads to poor prognosis and that Kpnβ1-knockdown markedly reduced SKBR-3 cell proliferation. Based on these findings, we believe that Kpnβ1 is related to Her2 and its knockdown reduces Her2 nuclear entry. To our knowledge, this is the first study to report the expression of Kpnβ1 and relevant pathological parameters in BC, and the effect on its prognosis. Our results revealed that Kpnβ1 knockdown reduced cell proliferation in SKBR-3 cell lines, and elucidated the relationship between Kpnβ1 and Her2 and its effect on nuclear entry. We identified the potential mechanism involved in the effect of Kpnβ1 on Her2 overexpression in BC cell proliferation.

One study limitation was the statistical parameters used in this study. Atypical statistical parameters should be used in future studies. Furthermore, experiments on Kpnβ1-knockdown in affected BC cells after blocking Her2 nuclear entry have not been fully demonstrated and therefore warrant further study to further uncover the mechanism.

Acknowledgements

This study was supported by the National Natural Science Foundation of China (no. 81672596), Nantong Science and Technology Project (no. MS22015058) and Nantong University Innovation Project (YKC15085).

References

1. Parkin DM, Bray F, Ferlay J and Pisani P: Global cancer statistics, 2002. CA Cancer J Clin 55: 74-108, 2005.
2. Jemal A, Siegel R, Xu J and Ward E: Cancer statistics, 2010. CA Cancer J Clin 60: 277-300, 2010.
3. Nakielny S and Dreyfuss G: Transport of proteins and RNAs in and out of the nucleus. Cell 99: 677-690, 1999.
4. Chook YM and Blobel G: Karyopherins and nuclear import. Curr Opin Struct Biol 11: 703-715, 2001.
5. Giri DK, Ali-Seyed M, Li LY, Lee DF, Ling P, Bartholomeusz G, Wang SC and Hung MC: Endosomal transport of ErbB-2: Mechanism for nuclear entry of the cell surface receptor. Mol Cell Biol 25: 11005-11018, 2005.
6. Lo HW, Ali-Seyed M, Wu Y, Bartholomeusz G, Hsu SC and Hung MC: Nuclear-cytoplasmic transport of EGFR involves receptor endocytosis, importin beta1 and CRM1. J Cell Biochem 98: 1570-1583, 2006.
7. Zhen Y, Sørensen V, Skjerpen CS, Haugsten EM, Jin Y, Wälchli S, Olsnes S and Wiedlocha A: Nuclear import of exogenous FGF1 requires the ER-protein LRRC59 and the importins Kpnα1 and Kpnβ1. Traffic 13: 650-664, 2012.
8. Mosammaparast N and Pemberton LF: Karyopherins: From nuclear-transport mediators to nuclear-function regulators. Trends Cell Biol 14: 547-556, 2004.
9. Altan B, Yokobori T, Mochiki E, Ohno T, Ogata K, Ogawa A, Yanai M, Kobayashi T, Luvsandagva B, Asao T, *et al*: Nuclear karyopherin-α2 expression in primary lesions and metastatic lymph nodes was associated with poor prognosis and progression in gastric cancer. Carcinogenesis 34: 2314-2321, 2013.
10. Grupp K, Habermann M, Sirma H, Simon R, Steurer S, Hube-Magg C, Prien K, Burkhardt L, Jedrzejewska K, Salomon G, *et al*: High nuclear karyopherin α 2 expression is a strong and independent predictor of biochemical recurrence in prostate cancer patients treated by radical prostatectomy. Mod Pathol 27: 96-106, 2014.
11. Huang L, Wang HY, Li JD, Wang JH, Zhou Y, Luo RZ, Yun JP, Zhang Y, Jia WH and Zheng M: KPNA2 promotes cell proliferation and tumorigenicity in epithelial ovarian carcinoma through upregulation of c-Myc and downregulation of FOXO3a. Cell Death Dis 4: e745, 2013.
12. Pavlou MP, Dimitromanolakis A, Martinez-Morillo E, Smid M, Foekens JA and Diamandis EP: Integrating meta-analysis of microarray data and targeted proteomics for biomarker identification: Application in breast cancer. J Proteome Res 13: 2897-2909, 2014.
13. Ikenberg K, Valtcheva N, Brandt S, Zhong Q, Wong CE, Noske A, Rechsteiner M, Rueschoff JH, Caduff R, Dellas A, *et al*: KPNA2 is overexpressed in human and mouse endometrial cancers and promotes cellular proliferation. J Pathol 234: 239-252, 2014.

14. Hu ZY, Yuan SX, Yang Y, Zhou WP and Jiang H: Pleomorphic adenoma gene 1 mediates the role of karyopherin alpha 2 and has prognostic significance in hepatocellular carcinoma. J Exp Clin Cancer Res 33: 61, 2014.
15. Ma S and Zhao X: KPNA2 is a promising biomarker candidate for esophageal squamous cell carcinoma and correlates with cell proliferation. Oncol Rep 32: 1631-1637, 2014.
16. van der Watt PJ, Maske CP, Hendricks DT, Parker MI, Denny L, Govender D, Birrer MJ and Leaner VD: The karyopherin proteins, Crm1 and karyopherin beta1, are overexpressed in cervical cancer and are critical for cancer cell survival and proliferation. Int J Cancer 124: 1829-1840, 2009.
17. Zhang P, Garnett J, Creighton CJ, Al Sannaa GA, Igram DR, Lazar A, Liu X, Liu C and Pollock RE: EZH2-miR-30d-KPNB1 pathway regulates malignant peripheral nerve sheath tumour cell survival and tumourigenesis. J Pathol 232: 308-318, 2014.
18. Martens-de Kemp SR, Nagel R, Stigter-van Walsum M, van der Meulen IH, van Beusechem VW, Braakhuis BJ and Brakenhoff RH: Functional genetic screens identify genes essential for tumor cell survival in head and neck and lung cancer. Clin Cancer Res 19: 1994-2003, 2013.
19. van der Watt PJ, Stowell CL and Leaner VD: The nuclear import receptor Kpnβ1 and its potential as an anticancer therapeutic target. Crit Rev Eukaryot Gene Expr 23: 1-10, 2013.
20. Nordgard SH, Johansen FE, Alnaes GI, Bucher E, Syvänen AC, Naume B, Børresen-Dale AL and Kristensen VN: Genome-wide analysis identifies 16q deletion associated with survival, molecular subtypes, mRNA expression, and germline haplotypes in breast cancer patients. Genes Chromosomes Cancer 47: 680-696, 2008.
21. Ross JS and Fletcher JA: The HER-2/neu oncogene in breast cancer: Prognostic factor, predictive factor, and target for therapy. Oncologist 3: 237-252, 1998.
22. Li LY, Chen H, Hsieh YH, Wang YN, Chu HJ, Chen YH, Chen HY, Chien PJ, Ma HT, Tsai HC, *et al*: Nuclear ErbB2 enhances translation and cell growth by activating transcription of ribosomal RNA genes. Cancer Res 71: 4269-4279, 2011.
23. Gucalp A, Gupta GP, Pilewskie ML, Sutton EJ and Norton L: Advances in managing breast cancer: A clinical update. F1000Prime Rep 6: 66, 2014.
24. Lu T, Bao Z, Wang Y, Yang L, Lu B, Yan K, Wang S, Wei H, Zhang Z and Cui G: Karyopherin β1 regulates proliferation of human glioma cells via Wnt/β-catenin pathway. Biochem Biophys Res Commun 478: 1189-1197, 2016.
25. Wang S, Zhao Y, Xia N, Zhang W, Tang Z, Wang C, Zhu X and Cui S: KPNβ1 promotes palmitate-induced insulin resistance via NF-κB signaling in hepatocytes. J Physiol Biochem 71: 763-772, 2015.
26. Lee Y, Jang AR, Francey LJ, Sehgal A and Hogenesch JB: KPNB1 mediates PER/CRY nuclear translocation and circadian clock function. eLife 4: e08647, 2015.
27. Bennett SM, Zhao L, Bosard C and Imperiale MJ: Role of a nuclear localization signal on the minor capsid proteins VP2 and VP3 in BKPyV nuclear entry. Virology 474: 110-116, 2015.
28. Sun C, Yu Z, Wang Y and Tao T: The importin protein karyopherin-β1 regulates the mice fibroblast-like synoviocytes inflammation via facilitating nucleus transportation of STAT3 transcription factor. Biochem Biophys Res Commun 471: 553-559, 2016.
29. Kuusisto HV and Jans DA: Hyper-dependence of breast cancer cell types on the nuclear transporter importin β1. Biochim Biophys Acta 1853: 1870-1878, 2015.
30. Angus L, van der Watt PJ and Leaner VD: Inhibition of the nuclear transporter, Kpnβ1, results in prolonged mitotic arrest and activation of the intrinsic apoptotic pathway in cervical cancer cells. Carcinogenesis 35: 1121-1131, 2014.
31. Kojima Y, Nakayama M, Nishina T, Nakano H, Koyanagi M, Takeda K, Okumura K and Yagita H: Importin β1 protein-mediated nuclear localization of death receptor 5 (DR5) limits DR5/tumor necrosis factor (TNF)-related apoptosis-inducing ligand (TRAIL)-induced cell death of human tumor cells. J Biol Chem 286: 43383-43393, 2011.
32. Kim YH, Ha S, Kim J and Ham SW: Identification of KPNB1 as a cellular target of aminothiazole derivatives with anticancer activity. ChemMedChem 11: 1406-1409, 2016.
33. van der Watt PJ, Ngarande E and Leaner VD: Overexpression of Kpnβ1 and Kpnα2 importin proteins in cancer derives from deregulated E2F activity. PLoS One 6: e27723, 2011.
34. Zhang P, Yang X, Ma X, Ingram DR, Lazar AJ, Torres KE and Pollock RE: Antitumor effects of pharmacological EZH2 inhibition on malignant peripheral nerve sheath tumor through the miR-30a and KPNB1 pathway. Mol Cancer 14: 55, 2015.
35. Cordo Russo RI, Béguelin W, Díaz Flaqué MC, Proietti CJ, Venturutti L, Galigniana N, Tkach M, Guzmán P, Roa JC, O'Brien NA, *et al*: Targeting ErbB-2 nuclear localization and function inhibits breast cancer growth and overcomes trastuzumab resistance. Oncogene 34: 3413-3428, 2015.